

## Article

# Human Health Risk Assessment of Heavy Metals and Nitrates Associated with Oral and Dermal Groundwater Exposure: The Poirino Plateau Case Study (NW Italy)

Daniele Cocca , Manuela Lasagna , Enrico Destefanis , Chiara Bottasso and Domenico Antonio De Luca 

Earth Sciences Department, University of Turin, Via Valperga Caluso 35, 10125 Turin, Italy; daniele.cocca@unito.it (D.C.); manuela.lasagna@unito.it (M.L.); enrico.destefanis@unito.it (E.D.); chiara.bottasso@edu.unito.it (C.B.)

\* Correspondence: domenico.deluca@unito.it

**Abstract:** The Poirino Plateau (northwestern Italy) presents high contamination of the shallow aquifer due to intense agricultural practices and industrial activities. Many inhabitants have exploited shallow wells for personal purposes, coming into contact with contaminants. The aims of this study were to characterize groundwater contamination by heavy metals and nitrates, assess the noncarcinogenic and carcinogenic health risks for oral and dermal exposure in different receptor groups (children, adults, workers) and compare the noncarcinogenic and carcinogenic risk results with the regulatory limits and, therefore, if the actual regulatory limits are able to detect all potential situations of risk. For this purpose, 18 monitoring wells were collected in July 2022, and chemical–physical parameters and heavy metals were detected. The chemical data confirm a relevant anthropogenic contamination by nitrate and heavy metals. The estimated health risks are much higher in children, for oral exposure rather than dermal exposure for all the substances. The comparison between the results of the human health risk assessment and those in respect of threshold values confirms the existence of a transition condition. This condition, with concentrations below regulatory limits and above the noncarcinogenic or carcinogenic limits, reveals that the regulatory limits are not able to identify all the potential risk situations for the population.

**Keywords:** groundwater; heavy metals; nitrates; risk assessment; Italy



check for updates

**Citation:** Cocca, D.; Lasagna, M.; Destefanis, E.; Bottasso, C.; De Luca, D.A. Human Health Risk Assessment of Heavy Metals and Nitrates Associated with Oral and Dermal Groundwater Exposure: The Poirino Plateau Case Study (NW Italy). *Sustainability* **2024**, *16*, 222. <https://doi.org/10.3390/su16010222>

Academic Editors: Chengcheng Li and Xubo Gao

Received: 10 October 2023

Revised: 11 December 2023

Accepted: 24 December 2023

Published: 26 December 2023



**Copyright:** © 2023 by the authors. Licensee MDPI, Basel, Switzerland. This article is an open access article distributed under the terms and conditions of the Creative Commons Attribution (CC BY) license (<https://creativecommons.org/licenses/by/4.0/>).

## 1. Introduction

Groundwater pollution via inorganic and organic compounds is considered a serious global environmental issue since groundwater resources represent the main sources of drinking and potable water worldwide [1]. Understanding the extent of local contamination is crucial to protect groundwater resources. Heavy metals exist naturally in the environment and could have toxic effects in urban and agricultural areas where groundwater is affected by anthropogenic pollution [2].

Several metals and main ions are essential for humans, with particular roles in metabolism, while also facilitating endocrine signals between organs. Excessive concentrations of certain substances may lead to serious health issues [3]. Concerning heavy metals, Ba and Cd can influence the urinary system [4], and Cr(VI) ingestion carries a high risk for stomach cancers [5]. Mn can affect the central nervous system, Ni induces decreased body and organ weights and Zn can impact the hematopoietic and immune systems [4]. Regarding the other ions, F is an essential micronutrient in the human brain; however, high concentrations in water may cause damage to teeth and bones [6]. NO<sub>3</sub> can influence the hematopoietic system with early clinical signs of methemoglobinemia in infants [4].

Human health risk assessments allow us to define health risks through the evaluation of negative effects that occur in a person following an exposure. Many studies highlight

greater noncarcinogenic and carcinogenic risks in women compared to men [7,8], particularly for pregnant women [9], as well as greater risks in children compared to adults [10–14]. Furthermore, oral exposure appears to have more risk effects than dermal exposure [15,16]. Urbanization and anthropogenic pressures cause a deterioration in water resources and associated increased health risks [17–19]. Some studies have also been conducted in Italy, mainly evaluating heavy metals and nitrates [2,20–22].

Health risk assessments have become a mere comparison with selected reference values used to represent or characterize actual health risks [23], a practice now widespread in this research area [9,11,13] due to application for administrative and regulatory purposes as needed [24]. In Italy, the observance of concentrations in groundwater bodies takes place through a comparison between the measured concentrations of individual substances and the regulatory limits. This practice does not allow the possible cases of risk for the population to be highlighted even in the absence of exceeding the regulatory limits; moreover, the sum of effects connected to multiple substances is not considered [24,25]. Risk assessment helps the correct and most sustainable remediation method for heavy metal pollution to be chosen, such as adsorption methods [26]. For NO<sub>3</sub> pollution, these assessments can contribute to defining a regional protocol for the prevention and mitigation of diffuse pollution [27]. For these reasons, it is essential to know the concentrations existing in the groundwater, understand and identify their origin but also evaluate the effects on human health when the concentrations are consumed over an extended period of time, given that they can potentially increase cancer risk.

The Poirino Plateau (northwestern Italy) presents high contamination of the shallow aquifer due to intense agricultural practices and industrial activities; the latter have mainly existed in the second half of the 20th century, with repeated exceedances of regulatory limits [28]. This sector constitutes a rural area where the aqueduct network does not reach a high number of isolated homes. In these contexts, deep wells used for drinking water purposes are often mixed with polluted shallow aquifers. Moreover, many people exploit numerous shallow wells for personal purposes, such as personal hygiene, domestic uses and market gardens. Nitrogen pollution shows variable concentrations in spatial and temporal distribution [29], typical of areas with a high degree of pollution [30].

The aims of this study were to (1) assess groundwater contamination by heavy metals and nitrates in the Poirino Plateau, (2) assess the noncarcinogenic and carcinogenic health risk for oral and dermal exposure in different receptor groups, (3) compare the non-carcinogenic and carcinogenic risk results with the regulatory limits and, therefore, determine whether the actual regulatory limits are able to detect all potential situations of risk for the population. This study aims to increase knowledge on this topic, laying the basis for groundwater resource management that is sustainable for human health.

## 2. Materials and Methods

### 2.1. Study Area

#### 2.1.1. Geological and Hydrogeological Setting

This study area is located in the central sector of the Piedmont region, with an area of 55 km<sup>2</sup>. This sector is divided into 4 municipalities (Chieri, Riva di Chieri, Poirino and Villanova d'Asti) with approximately 11,000 inhabitants. The area, located on the Poirino Plateau, is bordered by hills to the north, east and south [31].

As regards the geological setting, the Piedmont Po Plain consists of (I) Pre-Pliocene marine deposits (Eocene–Miocene), (II) Pliocene marine clays deposits (Pliocene), (III) Pliocene marine deposits (Pliocene), (IV) Villafranchian transitional deposits (Late Pliocene–Early Pleistocene), (V) Middle Pleistocene fluvial deposits and (VI) Holocene fluvial deposits. The latter two host a shallow, unconfined aquifer [31]. In particular, the Poirino Plateau was analyzed in several previous studies [32,33].

Six hydrogeological complexes can be summarized (Figure 1) according to the permeability and grain size features of the geological formations [31,34,35]. The complexes are briefly described below from bottom to top. Silty–clayey sediments (conglomerates of

the Cassano Spinola, marls of St. Agata Fossili and Gessoso–Solfifera Formations) represent the pre-Pliocene marine complex (Eocene–Miocene). The Pliocene marine complex (Lower–Middle Pliocene) consists of Lugagnano clays and Asti sands. The Lugagnano clays, represented by sandy-marly clays, constitute an aquiclude under the overlying Asti Sands. The Asti sands are represented by permeable sandy deposits. This complex corresponds to a multilayered aquifer system due to the overlapping permeable and impermeable sediment levels. The overlying Villafranchian Transitional Complex (Middle Pliocene–Lower Pleistocene) is represented by silty–clayey levels with alternating sandy and gravelly levels. The Villafranchian complex reaches its maximum thickness (approximately 200 m) in the central portion of the Poirino Plateau, hosting a multilayered aquifers with the thickness increasing from east to west. Based on its features, such as the reduced distribution of permeable deposits, this complex represents the less exploited area on the Poirino Plateau. The alluvial complex (Middle Pleistocene–Holocene) is represented by terraced fluvial deposits consist of silty, sandy and gravelly deposits with maximum thicknesses of 30 m.

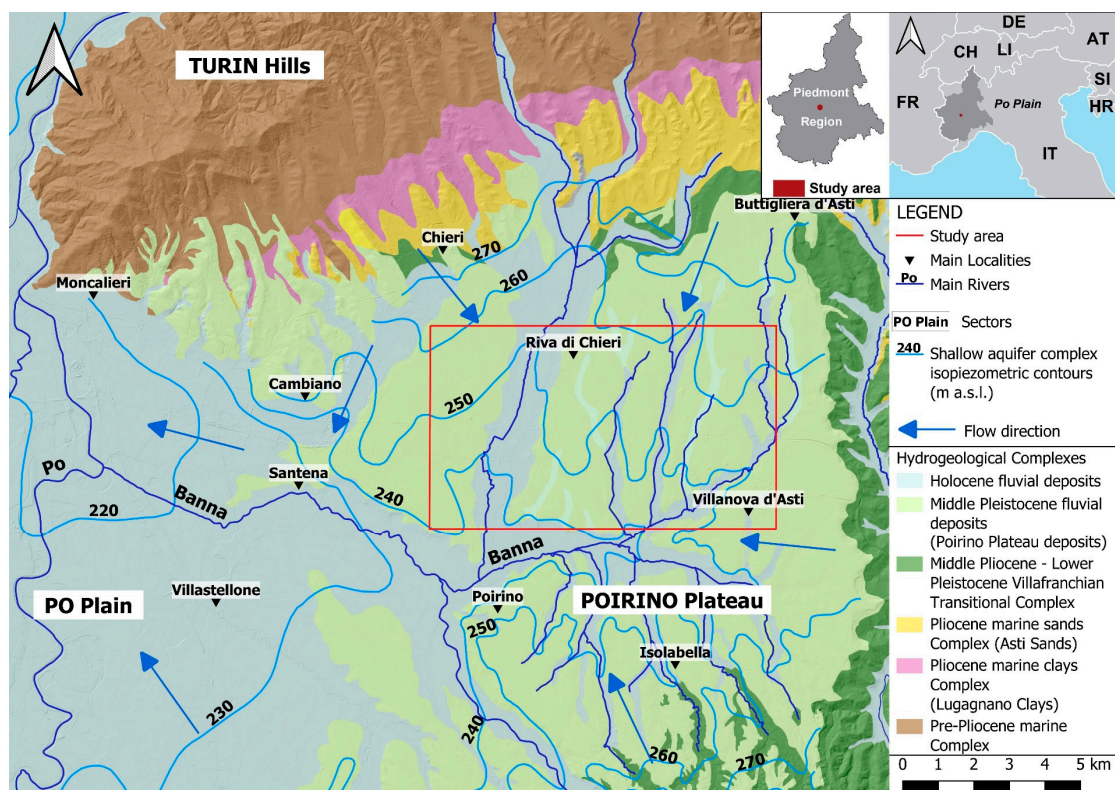


**Figure 1.** Map of the study area in the Piedmont Region (NW Italy), hydrogeological complexes and piezometric surface of the shallow aquifer in the Poirino Plateau (summer 2016) (modified from [31]).

The Middle Pleistocene–Holocene alluvial complex represents the shallow unconfined aquifer complex. The Villafranchian Transitional hydrogeological complex and the Pliocene Marine hydrogeological complex, that include confined and semiconfined aquifers, represent the deep aquifer complex. The main groundwater flow direction of the shallow aquifer complex on the Poirino Plateau is mainly flowing from east to west. In the present study area, the groundwater flow direction of the shallow aquifer complex is essentially from north to south (Figure 1). The water depth from the surface is between 1 and 10 m and mainly <5 m [31].

### 2.1.2. Hydrochemical and Land Use Setting

Regarding the hydrochemical features, the shallow aquifer complex of the Poirino Plateau shows calcium, magnesium sulphate and/or chloride facies and calcium and/or

magnesium bicarbonate facies, whereas the deep aquifer complex is characterized by more carbonatitic components [36]. The EC (electrical conductivity) of the shallow aquifer complex also reached values of 2000  $\mu\text{S}/\text{cm}$ ; meanwhile, in the deep aquifer complex, values below 600  $\mu\text{S}/\text{cm}$  were commonly observed. The groundwater of the Pliocene Marine complex is not affected by anthropogenic pollutants; in contrast, a high degree of nitrate diffuse pollution in the shallow aquifer complex in several previous studies was identified linked to intense agricultural activities [28,36,37]. Exceedances of regulatory limits were observed for Cr(VI) in the 1980s, with wastewater from noncontrolled activities [38]. Recently, the Regional Environmental Agency has detected repeated and discontinuous exceedances of regulatory limits for Cr(VI) [39].

The deep aquifer complex, that is intercepted with wells of depths exceeding 100 m (used for irrigation, industrial activities and drinking water), is often interconnected with the shallow aquifer. The wells capturing the shallow aquifer complex usually have depths of less than 30 m and are exploited mainly for irrigation activities and, secondarily, for domestic uses and personal purposes. Therefore, contaminants present in the shallow aquifer can contact humans via different pathways. In the present study area, irrigated arable areas are prevalent. The main industrial areas are located close to urban centers.

The industrial activities existing in the second half of the 20th century were mainly the metalworking industry. In this area, there are two important road and railway lines, both with a W–E orientation (Figure 2).

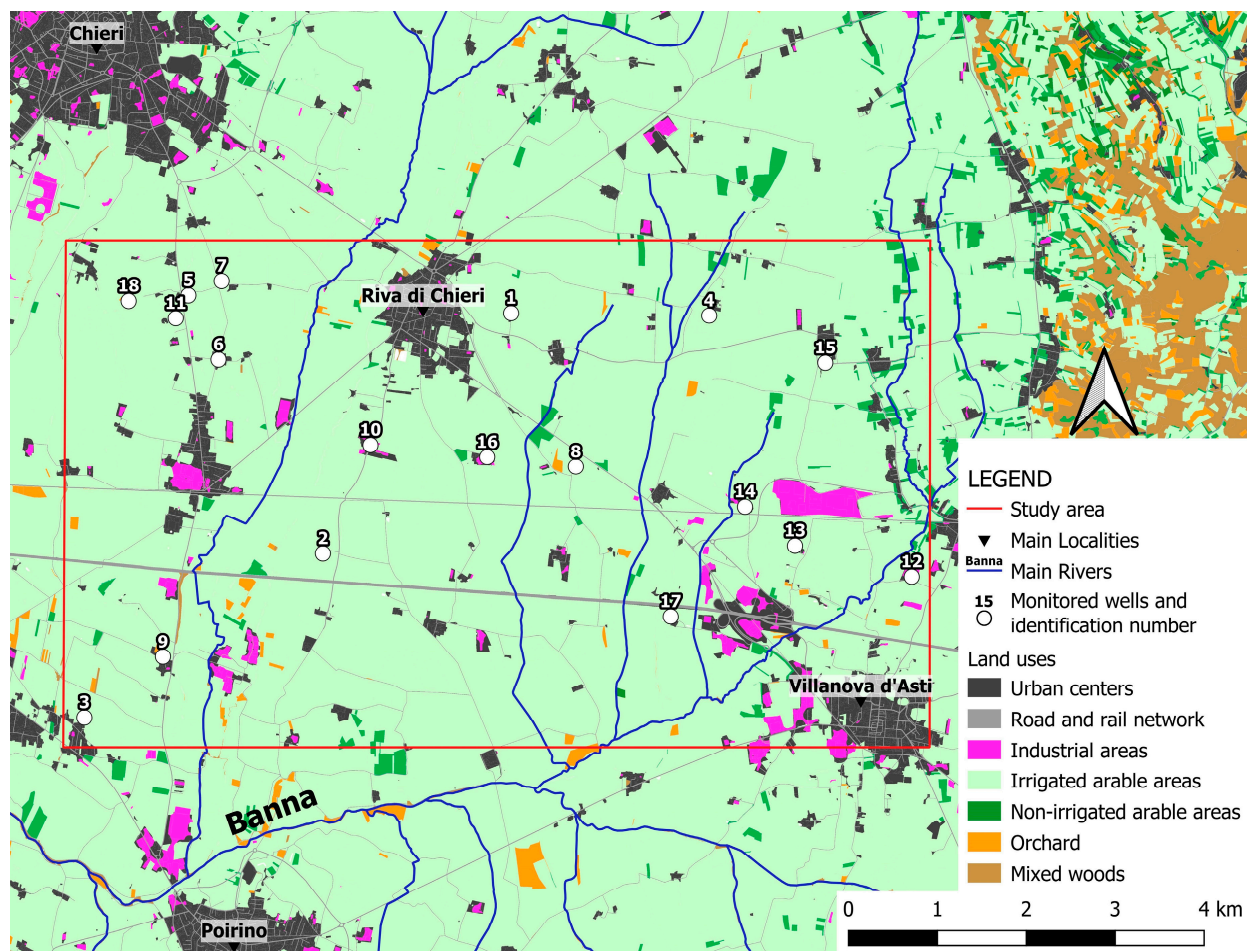


**Figure 2.** Land uses in the Piedmont Region. Corine land cover of the study area in the Piedmont Region (NW Italy), hydrogeological complexes and piezometric surface of the shallow aquifer [40].

## 2.2. Sampling and Analytical Procedures

A sampling campaign was performed in July 2022 to collect groundwater samples from the shallow aquifer, which corresponds to the central area of the Poirino Plateau. A total of 18 monitoring wells were collected (Figure 2). For each sampling point, polyethylene bottles (250–500 mL) for chemical–physical analysis of the main ions and heavy metals were used to collect two samples. Samples were collected using bottles and directly filled whilst awaiting water parameter stabilization. Bottles were filled until reaching the sealing disc, avoiding the presence of air inside the bottle, then stored in a refrigerator. During the sampling activities, the water table depth was measured while the parameters of electrical conductivity (EC), pH and total dissolved solids (TDS) were measured with a Hanna waterproof tester HI98130 measurer, and measurements were subsequently repeated in the laboratory (resolution and accuracy of EC: 0.01  $\mu\text{S}/\text{cm}$ , 2% F. S. (full scale); pH: 0.01 and 0.05; TDS: 0.01 g/L, 2% F.S.).

Hydrochemical analyses were performed in the laboratory of the Earth Sciences Department, University of Turin, while the ICP–MS analysis was performed in the Chemistry Department. For the lab analyses, the pH levels were measured with a Hanna Instrument H2211 pH/ORP meter calibrated with pH standards of 4.00, 7.00 and 10.00; the EC was measured with a Mettler Toledo Five Easy that was previously calibrated with a standard solution of KCl at 1462  $\mu\text{m}$  and 25 °C. Both instruments were equipped with automatic temperature compensation abilities. Metrohm 665 Dosimat using 0.1 N HCl as the titrating solution and a 100 mL sample was used for the determination of alkalinity ( $\text{HCO}_3$  and  $\text{CO}_3^{2-}$ ) with the acid–base titration method. Methyl orange was used as the color indicator. Ion chromatography for the anions and cations (F, Cl,  $\text{NO}_2$ , Br,  $\text{NO}_3$ ,  $\text{SO}_4$ , Na,  $\text{NH}_4$ , K, Mg, Ca) was used; in particular, chemical suppression ion chromatography was used for anions. The Metrohm IC883 and Metrohm 863 Autosampler systems equipped with Metrosep A-Supp4 250 and Metrosep C4 250 separation columns were used for anions and cations, respectively. The main ions were used for analytical quality control based on anion-cation charge balance with errors < 5%.

For the dispersed metal analysis, an aliquot of 50 mL was filtered on a 0.20  $\mu\text{m}$  filter to remove coarse particulate matter. In order to obtain a pH < 2, the resulting water was acidified with  $\text{HNO}_3$  (HP quality). The analysis was performed using an ICP Agilent 7500 to measure the quantity of Al, Ba, Cd, Co, Cu, Mn, Ni, Pb and Zn. The determination of Cr(VI) was carried out according to the EPA 218.7 method, which involves the use of ion chromatography associated with post-column derivatization with 1,5-diphenylcarbazide and a UV-Vis detector.

The chemical analyses conducted made it possible to characterize the shallow aquifer. In particular, the classification diagrams (i.e., Piper [41], Cl/Na,  $\text{NO}_3/\text{Cl}$  ratio and Cl) were created. For the mixing diagram with the  $\text{NO}_3/\text{Cl}$  ratio and Cl, the fields were taken from [42].

## 2.3. HPI Index

To define the degree of water contamination, the heavy metal pollution index (HPI) is frequently utilized [2,16]. This pollution index, which was defined by [43], represents the influence of heavy metals on groundwater quality. This index, that establishes a weightage ( $W_i$ ) between 0 and 1, is inversely proportional to the standard permissible value ( $S_i$ ) [44,45].

The HPI is defined in Equations (1) and (2) as follows:

$$\text{HPI} = \frac{\sum_{i=1}^n W_i Q_i}{\sum_{i=1}^n W_i} \quad (1)$$

where  $W_i$  correspond to the unit weight of the  $i$ th parameter;  $n$  is the number of heavy metals considered and  $Q_i$  is the sub-index of the  $i$ th parameter.  $Q_i$  is defined as follows:

$$Q_i = \sum_{i=1}^n \frac{|M_i - I_i|}{S_i - I_i} \times 100 \quad (2)$$

where  $S_i$  represents the highest permissible value for the  $i$ th parameter in relation to the water quality standard;  $I_i$  corresponds to the ideal value or permissible limit for the  $i$ th parameter; and  $M_i$  represents the considered metal value for the  $i$ th sample.  $W_i$  is set to  $1/S_i$  [46]. In accordance with the HPI results, the pollution degree was composed of three classes as follows: low (HPI < 50), medium (HPI 50–100) and high (HPI > 100) contamination [47].

#### 2.4. Human Health Risk Assessment

The noncarcinogenic and carcinogenic health risk levels in relation to the consumption of contaminated groundwater were determined through a health risk assessment. In this study, the populations were grouped into three groups: children, adults and workers (the latter having a lower exposure frequency than adults). The human health risk was evaluated for oral and dermal exposure.

The heavy metals Cr(VI), Cd and Pb are classified as carcinogenic pollutants by the International Agency for Research on Cancer (IARC), whereas the heavy metals Al, Ba, Co, Cu, Mn, Ni, Pb, Zn and  $\text{NO}_3$  and F ions are classified as noncarcinogenic [48]. In this research, carcinogenic risk assessments to evaluate Cr(VI), Cd and Pb impacts and the noncarcinogenic risk assessments to define Al, Ba, Cd, Co, Cr(VI), Cu, Mn, Ni, Pb, Zn and  $\text{NO}_3$ ,  $\text{NH}_4$  and F were applied.

##### 2.4.1. Noncarcinogenic Health Risk Assessment

Noncarcinogenic health risk assessments are adopted to quantify chronic daily intake (CDI) and hazard quotient (HQ). The chronic daily intake (CDI) of the substances was defined using Equations (3) and (4) [49,50]:

$$\text{CDI}_{oral} = \frac{C_i \times IR \times EF \times ED}{BW \times AT} \quad (3)$$

$$\text{CDI}_{dermal} = \frac{C_i \times SA \times Kp \times ET \times EF \times ED \times CF}{BW \times AT} \quad (4)$$

where  $C_i$  is the ion concentration ( $\mu\text{g/L}$ );  $IR$  corresponds to the ingestion rate (2 L per day for adults/workers, 1 L per day for children);  $SA$  represents the skin surface area (18,000  $\text{cm}^2$  for adults/workers, 7000  $\text{cm}^2$  for children);  $Kp$  represents the permeability coefficient ( $1 \times 10^{-3}$   $\text{cm/h}$ );  $ET$  represents the daily exposure time (0.4 h/day);  $EF$  represents the exposure frequency (350 days year for children and adults, 250 days year for workers);  $ED$  represents the exposure duration (24 years for adults/workers, 6 years for children);  $CF$  represents the conversion factor ( $2 \times 10^{-3}$   $\text{L/cm}^3$ );  $BW$  represents the average body weight of the consumers (70 kg for adults/workers, 15 kg for children); and  $AT$  represents the average time of the exposure (8760 days for adults/workers, 2190 days for children).

The assessment of noncarcinogenic health risks requires the hazard quotient (HQ) calculation, for both oral and dermal exposure, using Equation (5). HQ results higher than 1.0 indicate the existence of noncarcinogenic risk [50].

$$\text{HQ} = \frac{\text{CDI}}{\text{RfD}} \quad (5)$$

where  $\text{RfD}$  represents the reference dose (mg/kg per day) equal to 1/0.5 for Al, 0.2/0.1 for Ba,  $5 \times 10^{-4}/2.5 \times 10^{-4}$  for Cd,  $3 \times 10^{-4}/1.5 \times 10^{-4}$  for Co,  $3 \times 10^{-3}/1.5 \times 10^{-3}$  for Cr(VI), 0.04/0.02 for Cu, 0.06/0.03 for F, 0.14/0.07 for Mn, 0.02/0.01 for Ni, 0.48/0.24

for  $\text{NH}_4$ , 0.5/0.25 for  $\text{NO}_3$ , 0.0035/0.0017 for Pb, and 0.3/0.15 for Zn (oral and dermal exposure) [4].

The sum of the calculated HQ for each substance represents the overall potential for noncarcinogenic effects of several substances and is expressed as the hazard index (HI). No chronic risks are assumed to occur when HI is lower than one ( $\text{HI} < 1.0$ ) and possible chronic risk linked by groundwater ingestion could appear if HI is higher than one ( $\text{HI} \geq 1.0$ ) [49]. The total noncarcinogenic risks linked to exposure to inadequate drinking groundwater correspond to the sum of the oral hazard index and dermal hazard index [13,51].

#### 2.4.2. Carcinogenic Health Risk Assessment

The carcinogenic health risk index (R) is adopted to evaluate the potential carcinogenic health risk of contaminated groundwater using Equation (6):

$$R = CDI \times SF \quad (6)$$

where  $SF$  is the slope coefficient. A potential carcinogenic health risk occurs when the calculated value is greater than  $1 \times 10^{-6}$  for a single compound and  $1 \times 10^{-5}$  for the sum of compounds [24]. The  $SF$  for Cr(VI) corresponds to 0.5 mg/kg per day [52].

The chosen methods for the HPI index and human health risk assessment correspond to the most applied methods in similar studies and were therefore also selected for this study.

#### 2.5. Comparison of Human Health Risk Assessment and Threshold Values

The threshold values imposed by the Italian legislation [24,25] and the exceeding of the thresholds by the concentrations detected are highlighted in Table 1. In order to highlight the potential situations of risk for the population in the case of exceeding and not exceeding the regulatory limits, three maps were created (HQ  $\text{NO}_3$ , HI, R Cr(VI)).  $\text{NO}_3$  and Cr(VI) were chosen because they were the compounds with the greatest contribution to the noncarcinogenic and carcinogenic health risks, respectively.

**Table 1.** Chemical–physical data of 18 samples, regulatory limits and HPI. Values above the regulatory limits in italics.

ID	Locality	pH	EC ( $\mu\text{S}/\text{cm}$ )	HCO <sub>3</sub> (mg/L)	SO <sub>4</sub> (mg/L)	NO <sub>3</sub> (mg/L)	Cl (mg/L)	F (mg/L)	Ca (mg/L)	Mg (mg/L)	K (mg/L)	NH <sub>4</sub> (mg/L)	Na (mg/L)	Al ( $\mu\text{g}/\text{L}$ )	Cr(VI) ( $\mu\text{g}/\text{L}$ )	Mn ( $\mu\text{g}/\text{L}$ )	Co ( $\mu\text{g}/\text{L}$ )	Ni ( $\mu\text{g}/\text{L}$ )	Cu ( $\mu\text{g}/\text{L}$ )	Zn ( $\mu\text{g}/\text{L}$ )	Cd ( $\mu\text{g}/\text{L}$ )	Ba ( $\mu\text{g}/\text{L}$ )	Pb ( $\mu\text{g}/\text{L}$ )	HPI
		6–9	2500	/	250	50	250	1.5	/	/	/	0.5	200	200	5	50	50	20	1000	3000	5	/	10	
1	Riva di Chieri	8.2	587	224	9.3	19.6	14.1	4.2	84	19.2	3.1	<0.01	17.77	38.40	3.4	<0.05	<0.04	<1.5	<2.5	11	<0.06	43.0	<0.2	22.97
2	Riva di Chieri	8.1	597	224	28.6	29.7	18.8	<0.01	86	26.6	34.0	<0.01	30.72	<4	5.2	<0.05	1.7	<1.5	<2.5	<10	<0.06	26.0	<0.2	34.99
3	Poirino	7.7	976	150	62.1	51.7	133.7	<0.01	125	33.6	0.9	0.25	13.47	<4	<0.05	<0.05	<0.04	0.8	<2.5	13	<0.06	35.0	<0.2	0.34
4	Riva di Chieri	7.9	824	185	38.7	79.0	57.9	3.7	145	20.6	0.4	<0.01	24.79	<4	2.2	1.60	2.0	4.1	<2.5	701	<0.06	36.0	<0.2	16.73
5	Chieri	7.4	1247	312	379.0	1.1	20.5	0.2	253	52.4	13.2	<0.01	10.03	10.50	<0.05	5.50	<0.04	1.3	<2.5	<10	<0.06	21.0	<0.2	0.96
6	Chieri	8.0	711	233	82.2	34.0	36.9	0.3	103	26.6	42.5	<0.01	46.85	<4	2.1	<0.05	1.7	1.3	<2.5	<10	<0.06	44.0	<0.2	14.74
7	Chieri	7.9	483	220	24.6	12.5	16.1	2.1	87	27.5	0.6	<0.01	6.82	<4	30.5	<0.05	1.6	<1.5	<2.5	<10	<0.06	15.0	<0.2	204.69
8	Riva di Chieri	7.9	600	143	33.2	70.5	37.8	<0.01	101	21	0.3	0.15	13.93	<4	4.6	<0.05	1.7	0.6	2.6	<10	<0.06	18.2	<0.2	31.22
9	Poirino	7.9	777	219	45.6	60.6	16.7	<0.01	81	19.3	0.4	<0.01	8.12	<4	10.4	<0.05	1.9	0.2	<2.5	<10	<0.06	17.8	<0.2	69.93
10	Riva di Chieri	8.1	322	139	4.8	15.4	10.4	<0.01	61	15.1	0.2	<0.01	7.91	<4	14.2	<0.05	1.7	0.7	<2.5	<10	<0.06	3.0	<0.2	95.66
11	Chieri	7.9	427	191	19.3	6.3	19.6	2.4	96	24.1	0.5	<0.01	6.76	<4	39.0	<0.05	1.7	<1.5	<2.5	<10	<0.06	1.7	<0.2	261.71
12	Villanova d’Asti	8.0	442	163	7.1	29.6	24.7	<0.01	92	16.2	0.3	<0.01	11.45	<4	14.2	<0.05	1.6	<1.5	<2.5	<10	<0.06	15.0	<0.2	95.36
13	Villanova d’Asti	8.0	403	138	16.0	9.5	22.7	<0.01	77	13.3	0.3	1.25	12.20	<4	12.1	<0.05	1.6	<1.5	<2.5	<10	<0.06	10.6	<0.2	81.27
14	Villanova d’Asti	7.8	819	141	61.1	25.7	71.4	<0.01	135	28.1	1.1	<0.01	32.01	<4	<0.05	<0.05	<0.04	<1.5	<2.5	622	<0.06	31.0	<0.2	0.01
15	Villanova d’Asti	7.9	470	142	33.7	15.9	33.4	<0.01	112	16.7	0.2	0.80	17.07	<4	0.7	<0.05	<0.04	<1.5	<2.5	<10	<0.06	39.0	<0.2	4.70
16	Riva di Chieri	7.8	538	320	9.5	6.8	21.3	0.3	68	24.0	0.8	<0.01	15.58	<4	12.3	<0.05	1.7	<1.5	<2.5	10	<0.06	13.6	<0.2	82.62
17	Villanova d’Asti	8.2	352	203	8.7	0.3	0.8	<0.01	58	4.8	1.1	0.10	16.57	<4	1.9	<0.05	1.7	<1.5	<2.5	<10	<0.06	4.7	<0.2	12.86
18	Chieri	8.4	422	234	18.2	<0.05	5.2	<0.01	66	8.1	1.0	0.45	20.62	<4	2.0	1.30	1.6	<1.5	4.5	<10	<0.06	8.3	<0.2	13.62

### 3. Results and Discussion

#### 3.1. Physicochemical Characterization and HPI Results

The results of the chemical–physical analyses are reported in Table 1. The hydrochemical results permitted us to highlight differences in the mineralization conditions of the monitoring wells. The electrical conductivity shows a wide range of variation, between 322 and 1247  $\mu\text{S}/\text{cm}$ , while pH levels show alkaline values between 7.40 and 8.35. Both show a heterogeneous spatial distribution, i.e., without spatial trends but appearing as punctual anomalies.

In the Piper diagram (Figure 3), a large number of sample points plot within the calcium–bicarbonate facies, while only three samples plot within the calcium–chloride–sulfate facies. These three samples (nos. 3, 5 and 14) correspond to the samples with the highest electrical conductivity samples. The cation triangle shows low variability between samples, with a Ca/Mg ratio in favor of Ca. Reverse situation in the anion triangle with a ratio in favor of  $\text{HCO}_3$  and an influence of Cl.

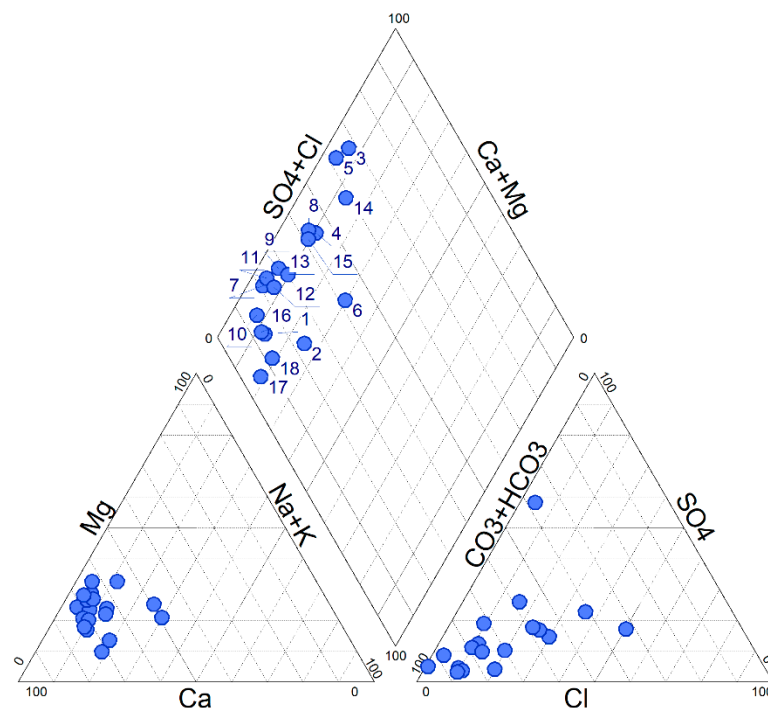


**Figure 3.** Piper diagram of the monitoring wells. Numbers correspond to identification number of samples.

The ions show a large range of variation.  $\text{HCO}_3$  shows a range of variation between 138 and 320 mg/L, with higher values in the northwestern sector, and Ca and Mg have values between 58 and 253 mg/L and between 5 and 52 mg/L, respectively.  $\text{NO}_3$  and Cl had ranges of variation between 0.05 and 79 and between 0.8 and 134 mg/L, respectively; however, these two ions showed similar spatial distributions. Na and  $\text{SO}_4$  showed values between 7 and 47 mg/L and between 5 and 379 mg/L, respectively. F was detected only in the northwestern and central sectors of the current study area with maximum values of 4.2 mg/L.  $\text{NH}_4$  was detected in two-thirds of the samples with a maximum value of 0.4 mg/L.  $\text{NO}_2$  was always lower than the detection limits. The heterogeneous spatial distribution is highlighted for all ions described herein.

The order of metal abundance concentrations in the overall groundwater samples of the current study area was as follows:  $\text{Zn} > \text{Ba} > \text{Cr(VI)} > \text{Al} > \text{Co} > \text{Ni} > \text{Mn} > \text{Cu}$ , whereas the concentrations of Cd and Pb were below the detection limits. Zn was detected only in one-third of samples with concentrations below 15  $\mu\text{g}/\text{L}$ , except for two samples in the eastern sector (nos. 4–7), with values up to 701  $\mu\text{g}/\text{L}$ . As concerns the other metals,

these were detected only in a few samples. Their maximum concentrations were as follows: Ba 44  $\mu\text{g/L}$ , Cr(VI) 39  $\mu\text{g/L}$ , Al 38.4  $\mu\text{g/L}$ , Co 2  $\mu\text{g/L}$ , Ni 4.1  $\mu\text{g/L}$ , Mn 5.5  $\mu\text{g/L}$ , and Cu 4.5  $\mu\text{g/L}$ . Additionally, the metals show a heterogeneous spatial distribution. The northwestern sector is often characterized by higher concentrations than other sectors for various metals, F and  $\text{NH}_4$ .

The molar ratio diagram of Cl/Na (Figure 4a) highlights a good correlation, showing a ratio of approximately 1, with only one sample with a ratio in favor of Cl (sample no. 3). The mixing diagram with the  $\text{NO}_3/\text{Cl}$  ratio and Cl (Figure 4b) suggests an anthropogenic origin of  $\text{NO}_3$  and Cl, related to sewage and manure inputs.

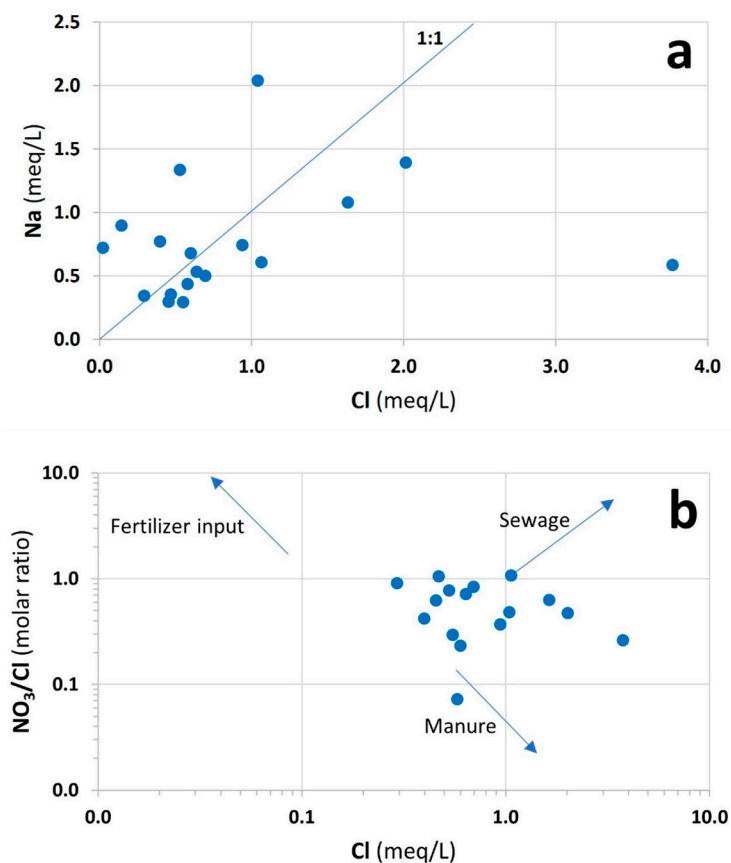


**Figure 4.** Correlation diagrams: (a) Cl vs. Na; (b)  $\text{NO}_3/\text{Cl}$  vs. Cl. For the  $\text{NO}_3/\text{Cl}$  vs. Cl, the fields were taken from [42].

Regarding the hydrochemical data, the heterogeneous spatial distribution with punctual anomalies of various ions, the absence of spatial trends, the contemporary presence of high and low concentrations of  $\text{NO}_3$  close to each other, the presence of high metal concentrations, the proportionality between EC and metals and the evidence of other hydrochemical diagrams suggest a relevant anthropogenic origin for  $\text{NO}_3$  and metals, originating from agricultural practices and the metalworking industry. Their concentrations are influenced by the characteristics of the aquifer, conditioning the oxidation–reduction processes. The HPI values ranged from 0.01 to 261.71 with an average value of 58.0 (Table S1 of the Supplementary Materials). Eleven samples belonged to the low category (nos. 1, 2, 3, 4, 5, 6, 8, 14, 15, 17, and 18), five belonged to the medium category (nos. 9, 10, 12, 13, and 16), and two belonged to the high category (nos. 7 and 11). The high HPI values were attributed essentially to Cr(VI). These values demonstrate that products of human activity impact the shallow aquifer in terms of heavy metal contamination, identifying a relevant degree of pollution in the present study area.

### 3.2. Human Health Risk Assessment

#### 3.2.1. Noncarcinogenic Risk Assessment

Noncarcinogenic risk (HQ) estimates for Al, Ba, Cd, Co, Cr(VI), Cu, Mn, Ni, Pb, Zn and NO<sub>3</sub>, NH<sub>4</sub> and F are described below. The HQ for the individual samples are reported in Table S2 of the Supplementary Materials. Cd and Pb were not detected and, therefore, were excluded from the assessment.

The order of HQ (mean values) for the oral pathway was NO<sub>3</sub> > F > Co > Cr(VI) > Fe > Zn > Ba > NH<sub>4</sub> > Ni > Cu > Mn > Al (Figure 5a). For the oral pathway of individual substances (HQ oral), 11 samples had HQ values greater than 1 in the children's group. For the adults' group, only five samples have HQ values higher than 1; meanwhile, for the workers' group, no samples reached the unit. Exceedances of unity are related to NO<sub>3</sub> and F (Figure 6a), while individual metals were less than 1 in all groups (Figure 6b).

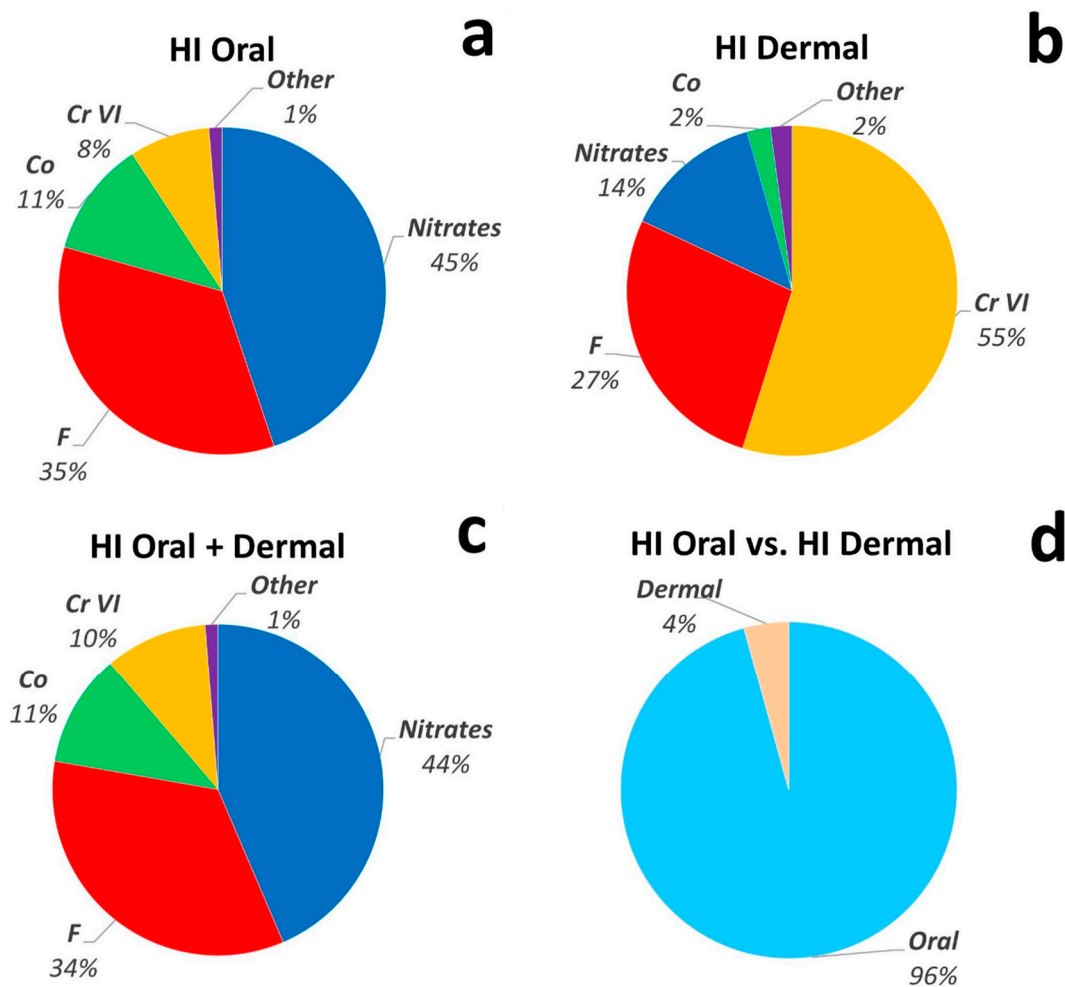


**Figure 5.** Average of the estimated noncarcinogenic risk for the 18 samples divided by substances and exposure: (a) HI oral; (b) HI dermal; (c) HI oral + dermal; (d) HI oral vs. dermal.

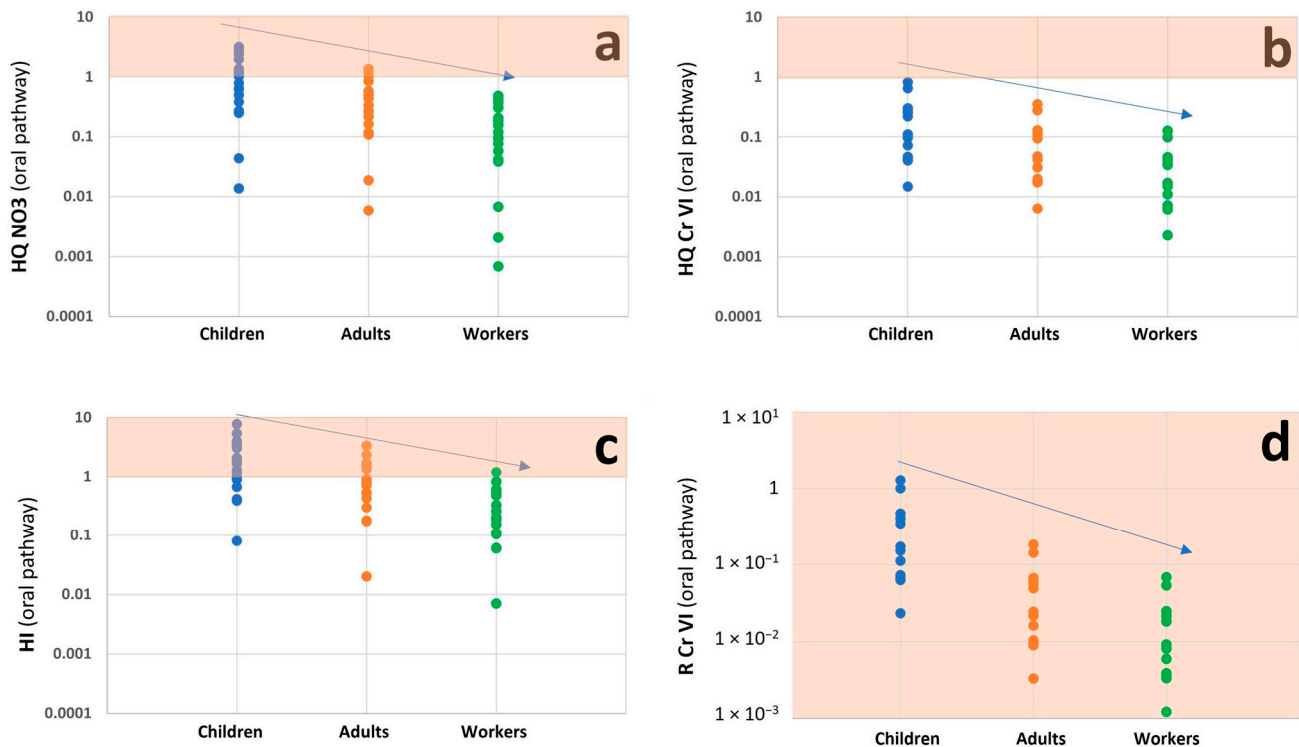


**Figure 6.** Exceedances of carcinogenic and noncarcinogenic risk limits for oral exposure divided by receptors: (a) HQ NO<sub>3</sub>; (b) HQ Cr(VI); (c) HI oral; (d) R Cr(VI). Risk fields in orange.

The order of HQ (mean values) for the dermal pathway was Cr(VI) > F > NO<sub>3</sub> > Co > Ni > Ba > Fe > Zn > Mn > NH<sub>4</sub> > Cu > Al (Figure 5b). For the dermal pathway of individual substances (HQ dermal), no samples reach the unit in all groups. The highest value of oral HQ (4.52) was obtained in the children's group for F influence, while the highest dermal HQ (0.22) was obtained for Cr(VI) influence, for sample nos. 1 and 11, respectively.

Considering the sum of the heavy metals for the oral pathway exclusively, two samples (nos. 7 and 11) show a higher value of 1. In percentage terms, the sum of heavy metals shows a rate of total risk ranging between 2 and 100% and is on average equal to 38%. For the dermal pathway, no sample reaches the unit; however, in percentage terms, the sum of heavy metals shows a rate on the total risk ranging between 9 and 100% and on average equal to 60%.

For the oral pathway of the sum of substances (HI oral), 12 samples had HI values greater than 1 in the children's group. For the adults' group, 6 samples have HI values higher than 1; meanwhile, for the workers' group, only 1 sample reached the unit (Figure 6c). For the dermal pathway of the sum of substances (HI dermal), no samples reached the unit in all groups.

The highest value of oral HI (7.74) was obtained in the children's group in sample no. 4, while the highest dermal HI (0.24) was observed in sample no. 11. The HQ and HI are much higher for oral exposure than for dermal exposure for all the substances and their sum. Total HI corresponding to the sum of HI oral and HI dermal (HI oral + dermal) shows an enormous similarity to oral HI in relation to the low influence of dermal HI on the total HI, on average equal to 4% (Figure 5c,d).

Therefore, the order of vulnerable receptors to toxic substances in the study area was found in the order of children > adults > workers for the individual substances and their sum in the oral, dermal and oral + dermal exposures. As a result, all three receptor groups may develop noncarcinogenic disorders in relation to the high values of HI emerged, mainly related to the ingestion of groundwater enriched with NO<sub>3</sub> and F and secondarily to heavy metals.

### 3.2.2. Carcinogenic Risk Assessment

R for the individual samples are reported in Table S3 of the Supplementary Materials. Human carcinogenic risk can be linked to heavy metals such as Cr(VI), Cd and Pb. In particular, the probability of developing health disorders may increase with prolonged exposure. As previously reported, Cd and Pb were not detected, and therefore, only Cr(VI) was considered. Cr(VI) was detected in all samples except nos. 3, 5 and 14.

For the oral pathway of Cr(VI) ( $R_{\text{oral}}$ ), all 15 samples had R values greater than  $1 \times 10^{-6}$  in the children's, adults' and workers' groups (Figure 6d), while for the dermal pathway ( $R_{\text{dermal}}$ ), all 15 samples had R values less than  $1 \times 10^{-6}$  in the children's, adults' and workers' groups. Total R corresponding to the cumulative of oral and dermal R ( $R_{\text{oral}} + R_{\text{dermal}}$ ) shows an irrelevant contribution from dermal exposure.

As a result, all three receptor groups may develop cancer diseases in relation to the high values of R that emerged, related to the ingestion of groundwater enriched with Cr(VI).

### 3.3. Comparison of Human Health Risk Assessment and Threshold Value Results

For the potential situations of risk for the population in the case of exceeding and not exceeding the regulatory limits were evaluated. Three maps were created for HQ  $\text{NO}_3$ , R Cr(VI) and HI (Figures 7–9) regarding the oral exposure of children to show the most precautionary situation. Due to the negligible dermal exposure, this was excluded from this comparison. As previously reported,  $\text{NO}_3$  and Cr(VI) were chosen as they were the compounds with the greatest contribution to the noncarcinogenic and carcinogenic health risks, respectively.

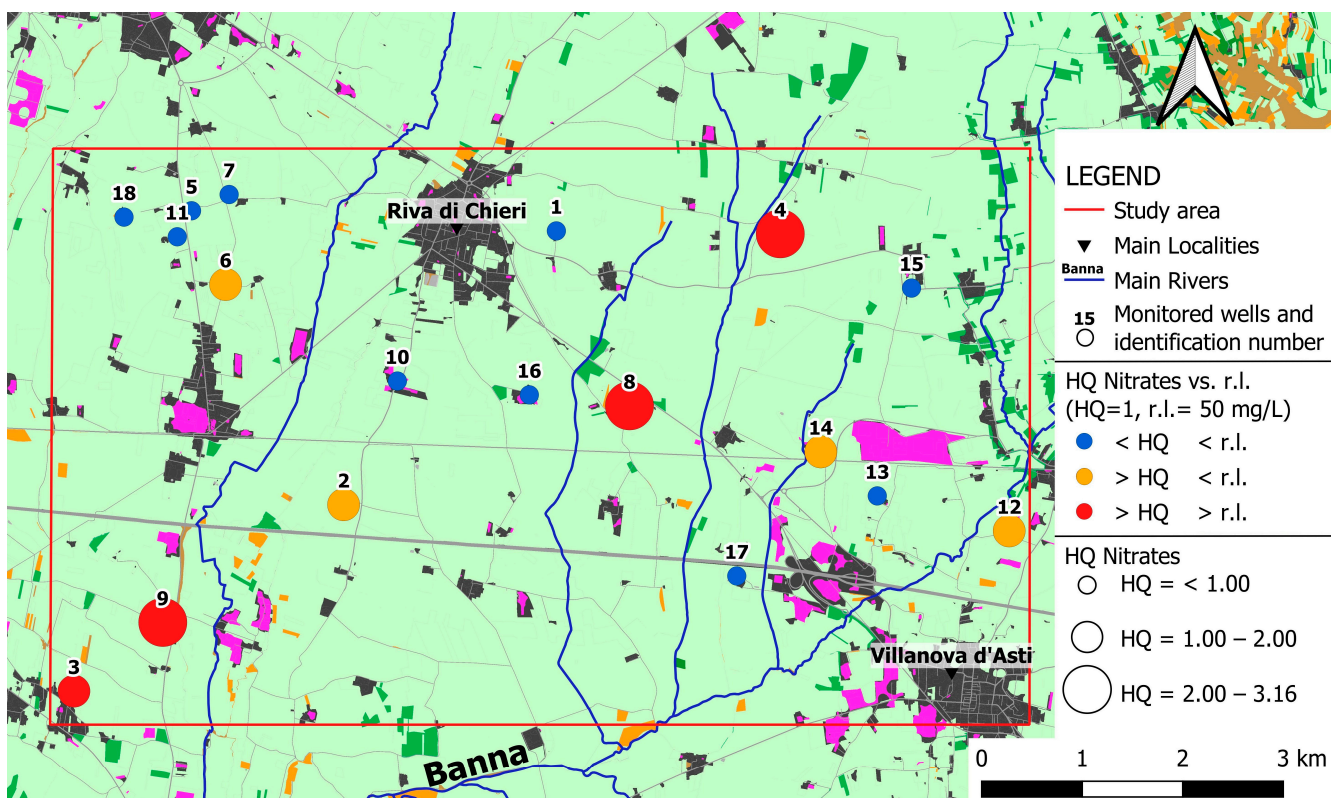


**Figure 7.** Representation of the comparison between HQ  $\text{NO}_3$  and regulatory limit for children's oral exposure. r.l.: regulatory limit, HQ maximum permissible value: 1. (Legend of the land use background is the same as in Figure 2).

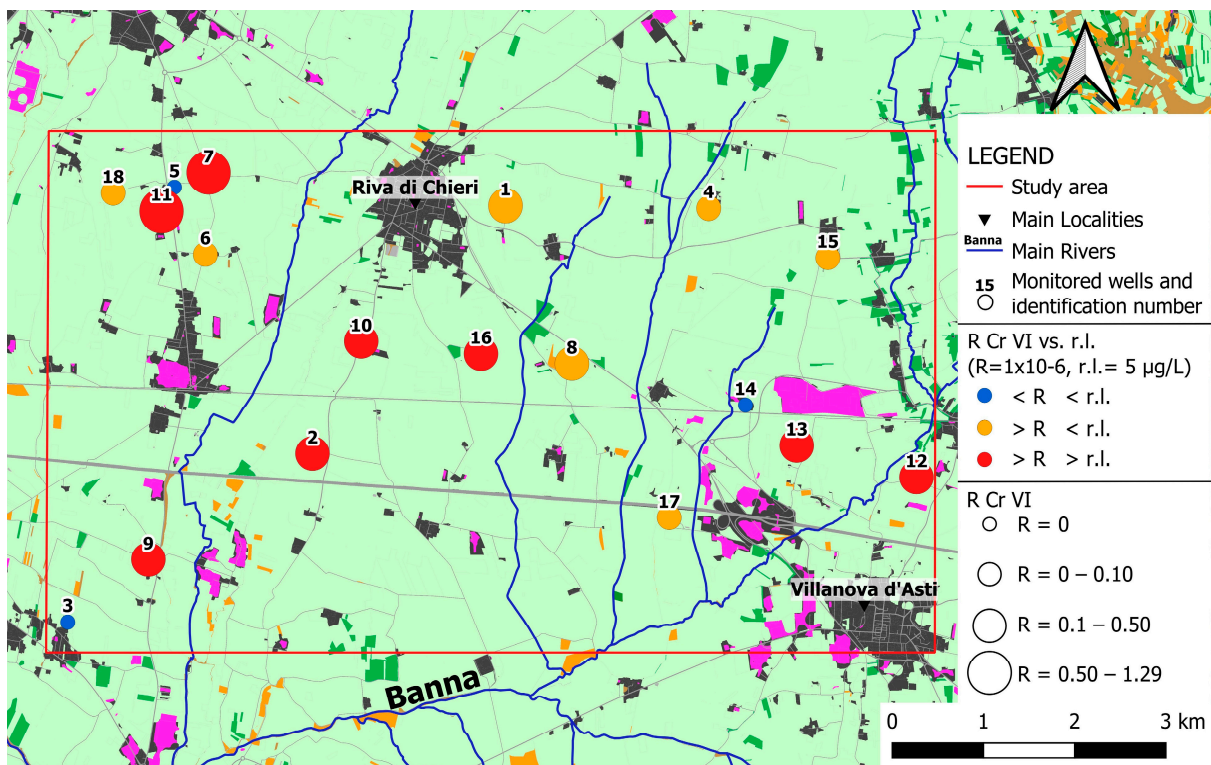


**Figure 8.** Representation of the comparison between R Cr(VI) and regulatory limit for children’s oral exposure. r.l.: regulatory limit. R maximum permissible value:  $1 \times 10^{-6}$ . (Legend of the land use background is the same as in Figure 2).

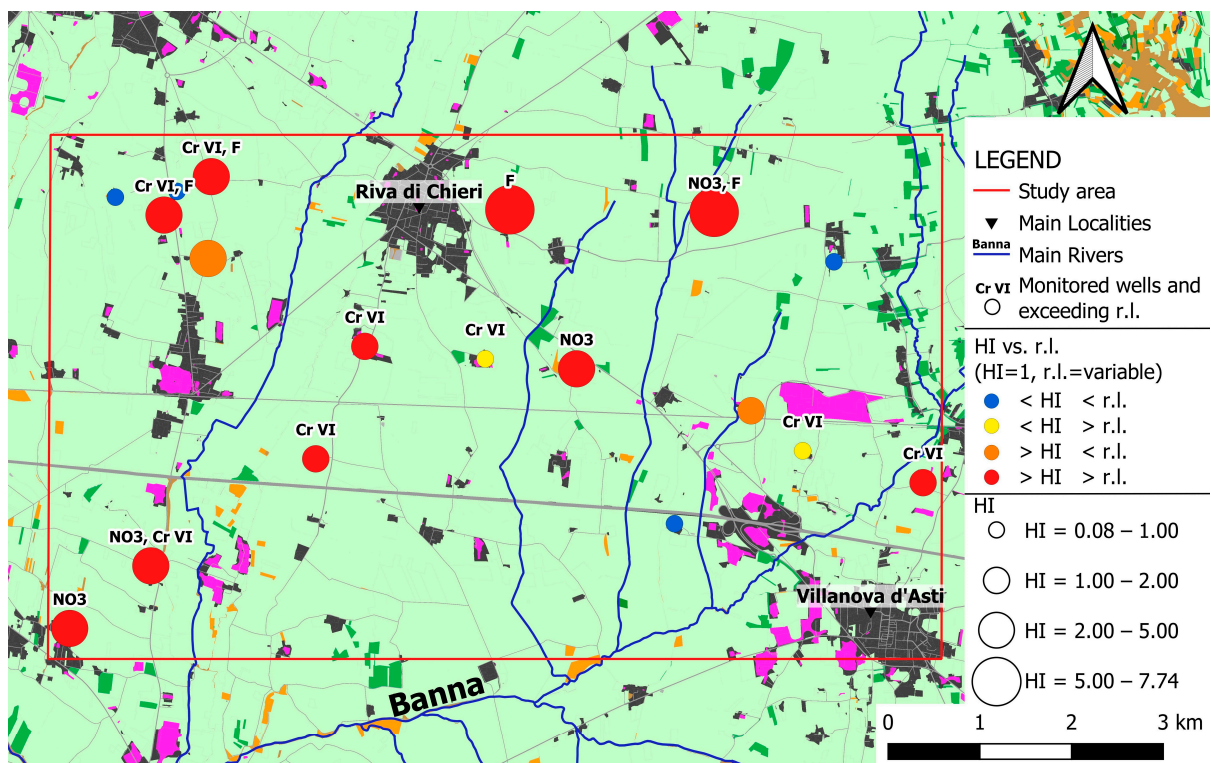


**Figure 9.** Representation of the comparison between HI (sum of substances) and regulatory limits for children’s oral exposure. r.l.: regulatory limit, HI maximum permissible value: 1. (Legend of the land use background is the same as in Figure 2).

Regarding the noncarcinogenic risk for NO<sub>3</sub> ingestion (Figure 7), only four samples showed concentrations above the regulatory limits until reaching 70.5 mg/L (nos. 3, 4, 8, 9). For these samples, HQ is above the unit and, therefore, noncarcinogenic risk exists. In the opposite condition, 10 samples show concentrations below the regulatory limits and HQ below the unit. For these samples, noncarcinogenic risk is negligible. However, four samples are in the transition condition corresponding with concentrations below the regulatory limits but HQ above the unit. Therefore, the health risk can be considered unacceptable for eight samples; meanwhile, with the use of regulatory limits, only four samples were identified.

Regarding the carcinogenic risk for Cr(VI) ingestion (Figure 8), eight samples showed concentrations above the regulatory limits until reaching 39 µg/L. For these samples, R is above  $1 \times 10^{-6}$ , and therefore, carcinogenic risk exists. In the opposite condition, three samples show concentrations below the regulatory limits (also below the detection limit) and R below the unit. For these samples, the carcinogenic risk is negligible. However, seven samples are in the transition condition previously described. Therefore, the health risk can be considered unacceptable for 15 samples; meanwhile, with the use of regulatory limits, only 8 samples were identified as unacceptable.

Regarding the noncarcinogenic risk for the cumulative of noncarcinogenic substances (Figure 9), 12 samples show concentrations above the regulatory limits, with exceedances for NO<sub>3</sub>, F and Cr(VI). In the opposite condition, four samples show concentrations below the regulatory limits and HI below the unit. However, four samples are in the transition conditions corresponding with concentrations below the regulatory limits but HI above the unit (nos. 6, 14) and concentrations above the regulatory limits but HI below the unit (nos. 13, 16). The exceeding of regulatory limits in the transition condition are in reference to Cr(VI) while the exceeding of units for the HI are in reference to NO<sub>3</sub>. Therefore, 12 samples were identified as unacceptable according to the regulatory limits and with the health risk assessment, 2 samples were added for a total of 14 samples to be identified as unacceptable.

Therefore, different conditions between the three health risk assessments exist. In particular, all four potential classes were detected (Figure 10).

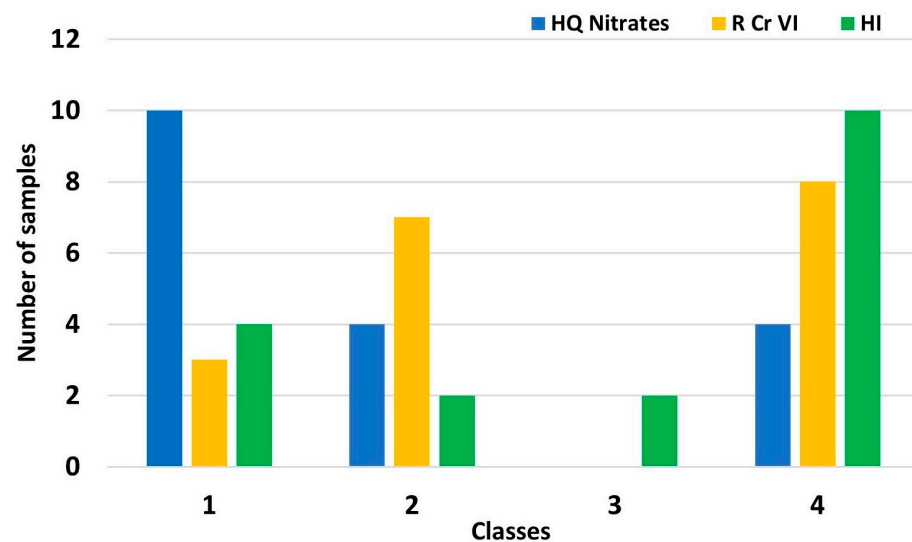


**Figure 10.** Subdivision of samples according to the comparison between the health risk results and regulatory limits compliance in the different four classes for children's oral exposure. Classes: (1) < r.l., no h.r.; (2) < r.l., h.r.; (3) > r.l., no h.r.; (4) > r.l., h.r.. (r.l.: regulatory limits, h.r.: health risk).

#### 4. Conclusions

Health risk assessments were applied to evaluate whether a condition of potential noncarcinogenic or carcinogenic risk exists even without exceeding the regulatory thresholds in relation to the high level of contamination of the shallow aquifer in the Poirino Plateau.

Chemical data confirm the anthropogenic origin of the heavy metals and NO<sub>3</sub> contamination, originating from agricultural practices and the metalworking industry, exacerbated by the characteristics of the aquifer as low transmissivity that conditions the oxidation–reduction processes. A relevant degree of pollution by heavy metals with the HPI index is confirmed.

Regarding the noncarcinogenic risk, the toxicity is primarily related to the ingestion of groundwater enriched with NO<sub>3</sub> and F and secondarily to heavy metals, while for dermal exposure, the toxicity is mainly related to Cr(VI). The noncarcinogenic and carcinogenic risks estimated are much higher for oral exposure than for dermal exposure for the substances and their sum. The vulnerable receptors to investigated substances for the noncarcinogenic and carcinogenic risk were found in the order of children > adults > workers, both for oral and dermal exposures, with the presence of risk in all groups. The carcinogenic risk for oral exposure is present in the samples where Cr(VI) is above the detection limit and for each receptor group. Twelve samples showed concentrations above the regulatory limits with exceedances for NO<sub>3</sub>, F and Cr(VI).

The comparison between the results of the human health risk assessment and in respect of threshold values confirms the existence of a transition condition corresponding to concentrations below the regulatory limits and above the noncarcinogenic or carcinogenic limits. These cases are situations that are not detected from the regulatory limits but represent a potential risk for human health. This situation reveals that for both the individual substances (HQ NO<sub>3</sub> and R Cr(VI)) and also for cumulative noncarcinogenic risk (HI), the current regulatory limits are not able to identify all the potential risk situations for the population.

According to these new findings, risk is present even if the regulatory thresholds are not exceeded. The usefulness of applying local characterizations of human health to simple comparisons with regulatory limits was confirmed. For a better assessment of the extent of the risk, it is advisable, not only for this study, to identify the possible sources of contamination, characterize temporal data through repeated sampling campaigns and to extend the analysis to other substances of recent interest and significant impact on human health, e.g., chlorinated solvents that are often associated with Cr(VI) contamination.

This research represents a successful application of an assessment of human health risk, which is useful for hydrogeologists working in comparable settings and for local authorities to increase the effectiveness of environmental protection, as well as for sustainable groundwater resource management.

**Supplementary Materials:** The following supporting information can be downloaded at: <https://www.mdpi.com/article/10.3390/su16010222/s1>. Table S1: statistical analysis of chemical-physical parameters; Table S2: non-carcinogenic risk (HQ) for the individual samples and parameters; Table S3: carcinogenic risk (R) for the individual samples.

**Author Contributions:** Conceptualization, D.C., M.L. and D.A.D.L.; methodology, D.C. and D.A.D.L.; software, D.C.; validation, D.C., M.L. and D.A.D.L.; formal analysis, D.C., M.L., D.A.D.L. and E.D.; investigation, D.C. and C.B.; resources, D.A.D.L.; data curation, D.C.; writing—original draft preparation, D.C.; writing—review and editing, D.A.D.L., M.L. and D.C.; visualization, D.C.; supervision, D.A.D.L. and M.L. All authors have read and agreed to the published version of the manuscript.

**Funding:** This research received no external funding.

**Institutional Review Board Statement:** Not applicable.

**Informed Consent Statement:** Not applicable.

**Data Availability Statement:** Data are contained within the article and Supplementary Materials.

**Conflicts of Interest:** The authors declare no conflicts of interest.

## References

1. Rapant, S.; Krčmová, K. Health risk assessment maps for arsenic groundwater content: Application of national geochemical databases. *Environ. Geochem. Health* **2007**, *29*, 131–141. [CrossRef] [PubMed]
2. Triassi, M.; Cerino, P.; Montuori, P.; Pizzolante, A.; Trama, U.; Nicodemo, F.; D’Auria, J.L.; De Vita, S.; De Rosa, E.; Limone, A. Heavy metals in groundwater of southern Italy: Occurrence and potential adverse effects on the environment and human health. *Int. J. Environ. Res. Public Health* **2023**, *20*, 1693. [CrossRef] [PubMed]
3. Nag, R.; O’Rourke, S.M.; Cummins, E. Risk factors and assessment strategies for the evaluation of human or environmental risk from metal(loid)s—A focus on Ireland. *Sci. Total Environ.* **2022**, *802*, 149839. [CrossRef] [PubMed]
4. US Environmental Protection Agency. Integrated Risk Information System. Available online: <http://www.epa.gov/iris/> (accessed on 10 September 2023).
5. Zhitkovich, A. Chromium in drinking water: Sources, metabolism, and cancer risks. *Chem. Res. Toxicol.* **2011**, *24*, 1617–1629. [CrossRef]
6. Edmunds, W.M.; Smedley, P.L. Groundwater quality: Focus on the fluoride problem in India. *Curr. Sci.* **2004**, *73*, 743–746.
7. Li, J.; Sun, C.; Chen, W.; Zhang, Q.; Zhou, S.; Lin, R.; Wang, Y. Groundwater Quality and Associated Human Health Risk in a Typical Basin of the Eastern Chinese Loess Plateau. *Water* **2022**, *14*, 1371. [CrossRef]
8. Zhai, Y.Z.; Zhao, X.B.; Teng, Y.G.; Li, X.; Zhang, J.J.; Wu, J.; Zuo, R. Groundwater nitrate pollution and human health risk assessment by using HHRA model in an agricultural area, NE China. *Ecotoxicol. Environ. Saf.* **2017**, *137*, 130–142. [CrossRef]
9. Zhang, Q.; Qian, H.; Xu, P.; Li, W.; Feng, W.; Liu, R. Effect of hydrogeological conditions on groundwater nitrate pollution and human health risk assessment of nitrate in Jiaokou Irrigation District. *J. Clean. Prod.* **2021**, *298*, 126783. [CrossRef]
10. Badeenezhad, A.; Radfard, M.; Abbasi, F.; Jurado, A.; Bozorginia, M.; Jalili, M.; Soleimani, H. Effect of land use changes on non-carcinogenic health risks due to nitrate exposure to drinking groundwater. *Environ. Sci. Pollut. Res.* **2021**, *28*, 41937–41947. [CrossRef]
11. Nsabimana, A.; Li, P.; He, S.; He, X.; Khorshed Alam, S.M.; Fida, M. Health Risk of the Shallow Groundwater and Its Suitability for Drinking Purpose in Tongchuan, China. *Water* **2021**, *13*, 3256. [CrossRef]
12. Zhang, Q.Y.; Xu, P.P.; Qian, H.; Yang, F.X. Hydrogeochemistry and fluoride contamination in Jiaokou Irrigation District, Central China: Assessment based on multivariate statistical approach and human health risk. *Sci. Total Environ.* **2020**, *741*, 140460. [CrossRef] [PubMed]
13. Xiao, Y.; Liu, K.; Hao, Q.; Xiao, D.; Zhu, Y.; Yin, S.; Zhang, Y. Hydrogeochemical insights into the signatures, genesis and sustainable perspective of nitrate enriched groundwater in the piedmont of Hutuo watershed, China. *Catena* **2022**, *212*, 106020. [CrossRef]
14. Cai, K.; Li, C.; Song, Z.; Gao, X.; Wu, M. Pollution and health risk assessment of carcinogenic elements As, Cd, and Cr in multiple media—A case of a sustainable farming area in China. *Sustainability* **2019**, *11*, 5208. [CrossRef]
15. Wu, J.; Sun, Z. Evaluation of Shallow Groundwater Contamination and Associated Human Health Risk in an Alluvial Plain Impacted by Agricultural and Industrial Activities, Mid-west China. *Expo. Health* **2016**, *8*, 311–329. [CrossRef]
16. Moldovan, A.; Hoaghia, M.A.; Kovacs, E.; Mirea, I.C.; Keneszy, M.; Arghir, R.A.; Petculescu, A.; Levei, E.A.; Moldovan, O.T. Quality and Health Risk Assessment Associated with Water Consumption—A Case Study on Karstic Springs. *Water* **2020**, *12*, 3510. [CrossRef]
17. Jat Baloch, M.Y.; Zhang, W.; Shoumik, B.A.A.; Nigar, A.; Elhassan, A.A.M.; Elshekh, A.E.A.; Bashir, M.O.; Mohamed Salih Ebrahim, A.F.; Adam Mohamed, K.A.; Iqbal, J. Hydrogeochemical Mechanism Associated with Land Use Land Cover Indices Using Geospatial, Remote Sensing Techniques, and Health Risks Model. *Sustainability* **2022**, *14*, 16768. [CrossRef]
18. Mi, W.; Zhang, M.; Li, Y.; Jing, X.; Pan, W.; Xing, X.; Xiao, C.; He, Q.; Bi, Y. Spatio-Temporal Pattern of Groundwater Nitrate-Nitrogen and Its Potential Human Health Risk in a Severe Water Shortage Region. *Sustainability* **2023**, *15*, 14284. [CrossRef]
19. Liu, Q.; Cheng, Y.; Fan, C. Pollution Characteristics and Health Exposure Risks of Heavy Metals in River Water Affected by Human Activities. *Sustainability* **2023**, *15*, 8389. [CrossRef]
20. Zhao, Y.; De Maio, M.; Suozzi, E. Assessment of Groundwater Potential Risk by Agricultural Activities, in North Italy. *Int. J. Environ. Sci. Dev.* **2013**, *4*, 3. [CrossRef]
21. Rufino, F.; Busico, G.; Cuoco, E.; Muscariello, L.; Calabrese, S.; Tedesco, D. Geochemical characterization and health risk assessment in two diversified environmental settings (Southern Italy). *Environ. Geochem. Health* **2022**, *44*, 2083–2099. [CrossRef]
22. Tiwari, A.K.; Suozzi, E.; Fiorucci, A.; Lo Russo, S. Assessment of groundwater geochemistry and human health risk of an intensively cropped alluvial plain, NW Italy. *Hum. Ecol. Risk Assess.* **2020**, *27*, 825–845. [CrossRef]
23. Sarigiannis, D.A.; Karakitsios, S.; Handakas, E.; Simou, K.; Solomou, E.; Gotti, A. Integrated exposure and risk characterization of bisphenol-A in Europe. *Food Chem. Toxicol.* **2016**, *98*, 134–147. [CrossRef] [PubMed]
24. D. Lgs. 152 del 03/04/2006 Norme in Materia Ambientale, G.U. n. 88 14/4/2006—Suppl. Ord. N. 96. 2006; Parlamento Italiano: Rome, Italy, 2006.
25. D. Lgs. 31 del 02/02/2001 Attuazione Della Direttiva 98/83/CE Relativa Alla Qualità Delle Acque Destinate Al Consumo Umano, G.U. n. 52 03/03/2001—Suppl. Ord. N. 41.2001; Parlamento Italiano: Rome, Italy, 2001.

26. Lu, B.; Chen, C.; Li, W.; Liu, H.; Liu, L.; Deng, S.; Li, Y. Effective removal of Cr(VI) from aqueous solution through adsorption and reduction by magnetic S-doped Fe-Cu-La trimetallic oxides. *J. Environ. Chem. Eng.* **2022**, *10*, 107433. [CrossRef]
27. D. 91/676/CEE 12/12/1991; Relating to the Protection of Waters from Pollution Caused by Nitrates from Agricultural Sources. European Environment Agency: Copenhagen, Denmark, 1991.
28. Lasagna, M.; De Luca, D.A.; Franchino, E. The role of physical and biological processes in aquifers and their importance on groundwater vulnerability to nitrate pollution. *Environ. Earth Sci.* **2016**, *75*, 961. [CrossRef]
29. Cocca, D.; Lasagna, M.; Marchina, C.; Brombin, V.; Santillan-Quiroga, L.M.; De Luca, D.A. Assessment of the groundwater recharge processes of a shallow and deep aquifer system (Maggiore Valley, Northwest Italy): A hydrogeochemical and isotopic approach. *Hydrogeol. J.* **2023**. [CrossRef]
30. Wang, X.; Xu, Y.J.; Zhang, L. Watershed scale spatiotemporal nitrogen transport and source tracing using dual isotopes among surface water, sediments and groundwater in the Yiluo River Watershed, Middle of China. *Sci. Total Environ.* **2022**, *833*, 155180. [CrossRef] [PubMed]
31. De Luca, D.A.; Lasagna, M.; Debernardi, L. Hydrogeology of the Western Po Plain (Piedmont, NW Italy). *J. Maps.* **2020**, *16*, 265–273. [CrossRef]
32. Forno, M.G. Geological study of the Poirino plateau (Turin). *Geogr. Fis. E Din. Quat.* **1982**, *5*, 129–162. (In Italian)
33. Doglione, A.; Forno, M.G.; Gattiglio, M. New morphological, stratigraphic, structural and pedological data on the T. Traversola deformation zone recent evolution (Asti, Piedmont). *Ital. J. Quat. Sci.* **2011**, *24*, 101–103.
34. Bortolami, G.; Braga, G.; Colombetti, A.; Dal Pra, A.; Francani, V.; Francavilla, F.; Giuliano, G.; Manfredini, M.; Pellegrini, M.; Petrucci, F.; et al. Hydrogeological features of the Po Valley (Northern Italy). In Proceedings of the IAHS Conference on Hydrogeology of Great Sedimentary Basins, Budapest, Hungary, 31 May–5 June 1976.
35. Lasagna, M.; Caviglia, C.; De Luca, D.A. Simulation modeling for groundwater safety in an overexploitation situation: The Maggiore Valley context (Piedmont, Italy). *Bull. Eng. Geol. Environ.* **2014**, *73*, 341–355. [CrossRef]
36. Vigna, B.; Fiorucci, A.; Ghielmi, M. Relations between stratigraphy, groundwater flow and hydrogeochemistry in Poirino Plateau and Roero areas of the Tertiary Piedmont Basin, Italy. *Mem. Descr. Carta Geol. D’it.* **2010**, *XC*, 267–292.
37. Lasagna, M.; De Luca, D.A.; Franchino, E. Nitrate contamination of groundwater in the western Po Plain (Italy): The effects of groundwater and surface water interactions. *Environ. Earth Sci.* **2016**, *75*, 240. [CrossRef]
38. Campigotto, L. Hydrogeochemical Study of the North-Western Sector of the Poirino Plateau. Master’s Thesis, University of Turin, Turin, Italy, 1989. (In Italian).
39. ARPA Piemonte. ARPA Activities in the Management of the Groundwater Monitoring Network in the Three Years 2009–2011. Proposal for Classification of the Quality Status of Groundwater Bodies Pursuant to Decree 260/2010. Struttura Specialistica Qualità Delle Acque. 2012. Available online: [https://www.arpa.piemonte.it/approfondimenti/temi-ambientali/acqua/acque-sotterranee/Relazione\\_sotterranee\\_triennio20092011\\_rev\\_finale\\_con\\_allegati.pdf](https://www.arpa.piemonte.it/approfondimenti/temi-ambientali/acqua/acque-sotterranee/Relazione_sotterranee_triennio20092011_rev_finale_con_allegati.pdf) (accessed on 8 October 2023). (In Italian).
40. Regione Piemonte. Land Cover Piemonte: Land Use Classification 2010 (Raster). 2010. Available online: [https://www.geoportale.piemonte.it/geonetwork/srv/ita/catalog.search#/metadata/r\\_piemon:4647f5d5-ed39-428d-a84b-8916e77e8f4c](https://www.geoportale.piemonte.it/geonetwork/srv/ita/catalog.search#/metadata/r_piemon:4647f5d5-ed39-428d-a84b-8916e77e8f4c) (accessed on 22 September 2023).
41. Piper, A.M. A Graphic Procedure in the Geochemical Interpretation of Water-Analyses. *Eos Trans. Am. Geophys. Union* **1944**, *25*, 914–928. [CrossRef]
42. Su, C.; Zhang, F.; Cui, X.; Chen, Z.; Zheng, Z. Source characterization of nitrate in groundwater using hydrogeochemical and multivariate statistical analysis in the Muling-Xingkai Plain, Northeast China. *Environ. Monit. Assess.* **2020**, *192*, 456. [CrossRef] [PubMed]
43. Mohan, S.V.; Nithila, P.; Reddy, S.J. Estimation of Heavy Metal in Drinking Water and Development of Heavy Metal Pollution Index. *J. Environ. Sci. Health* **1996**, *A-31*, 283–289. [CrossRef]
44. Prasad, B.; Sangita, K. Heavy Metal Pollution Index of Ground Water of an Abandoned Open Cast Mine Filled with Fly Ash: A Case Study. *Mine Water Environ.* **2008**, *27*, 265–267. [CrossRef]
45. Milivojević, J.; Krstić, D.; Šmit, B.; Đekić, V. Assessment of Heavy Metal Contamination and Calculation of Its Pollution Index for Uglješnica River, Serbia. *Bull. Environ. Contam. Toxicol.* **2016**, *97*, 737–742. [CrossRef] [PubMed]
46. Rajkumar, H.; Naik, P.K.; Rishi, M.S. A new indexing approach for evaluating heavy metal contamination in groundwater. *Chemosphere* **2019**, *245*, 125598. [CrossRef]
47. Saleh, H.N.; Panahande, M.; Yousefi, M.; Asghari, F.B.; Conti, G.O.; Talaee, E.; Mohammadi, A.A. Carcinogenic and Noncarcinogenic Risk Assessment of Heavy Metals in Groundwater Wells in Neyshabur Plain, Iran. *Biol. Trace Elem. Res.* **2018**, *190*, 251–261. [CrossRef]
48. IARC (International Agency for Research on Cancer). World Cancer Report. Available online: <http://www.iarc.fr/en/publications/books/wcr/wcr-order.php> (accessed on 22 September 2023).
49. US Environmental Protection Agency. Baseline Human Health Risk Assessment. Available online: [https://hero.epa.gov/hero/index.cfm/reference/details/reference\\_id/786143](https://hero.epa.gov/hero/index.cfm/reference/details/reference_id/786143) (accessed on 10 September 2023).
50. US Environmental Protection Agency. *Risk Assessment Guidance for Superfund Volume I: Human Health Evaluation Manual (Part E)*; USEPA: Washington, DC, USA, 2004. Available online: [https://www.epa.gov/sites/production/files/2015-09/documents/part\\_e\\_final\\_revision\\_10-03-07.pdf](https://www.epa.gov/sites/production/files/2015-09/documents/part_e_final_revision_10-03-07.pdf) (accessed on 7 October 2023).

51. Hossain, M.; Patra, P.K. Contamination zoning and health risk assessment of trace elements in groundwater through geostatistical modelling. *Ecotoxicol. Environ.* **2020**, *189*, 110038. [[CrossRef](#)]
52. California Office of Environmental Health Hazard Assessment. Available online: <https://oehha.ca.gov/chemicals/chromium-hexavalent> (accessed on 22 September 2023).

**Disclaimer/Publisher's Note:** The statements, opinions and data contained in all publications are solely those of the individual author(s) and contributor(s) and not of MDPI and/or the editor(s). MDPI and/or the editor(s) disclaim responsibility for any injury to people or property resulting from any ideas, methods, instructions or products referred to in the content.